

Charge Resonance Character in the Charge Transfer State of Bianthrils: Effect of Symmetry Breaking on Time-Resolved Near-IR Absorption Spectra

Tomohisa Takaya,^{†,‡} Satyen Saha,^{†,§} Hiro-o Hamaguchi,[†] Moloy Sarkar,^{||}
Anunay Samanta,^{||} and Koichi Iwata^{*,⊥}

Department of Chemistry, School of Science, The University of Tokyo, 7-3-1 Hongo, Bunkyo-ku, Tokyo 113-0033, Japan, School of Chemistry, University of Hyderabad, Hyderabad 500 046, India, and Research Centre for Spectrochemistry, School of Science, The University of Tokyo, 7-3-1 Hongo, Bunkyo-ku, Tokyo 113-0033, Japan

Received: January 4, 2006; In Final Form: February 23, 2006

We study the effects of symmetry breaking on the photogenerated intramolecular charge transfer (CT) state of 9,9'-bianthrilyl (BA) with femtosecond time-resolved near-IR spectroscopy. The time-resolved near-IR spectra are measured in acetonitrile for a symmetric substituted derivative of 10,10'-dicyano-9,9'-bianthrilyl (DCBA) and asymmetric substituted derivatives of 10-cyano-9,9'-bianthrilyl (CBA) and 9-(*N*-carbazolyl)anthracene (C9A), as well as nonsubstituted BA. The transient near-IR absorption spectrum of each compound at 0 ps has a locally excited (LE) absorption band, which agrees with the transient absorption band of the corresponding monomer unit. At 3 ps after the photoexcitation, the symmetric compounds show a broad charge transfer (CT) absorption band, whereas no absorption peak appears in the spectra of the asymmetric compounds. The broad CT absorption at 1250 nm only observed for the symmetric compounds can be attributed to the charge resonance transition associated with two equivalent charge separated states.

Introduction

The photoinduced intramolecular charge transfer in 9,9'-bianthrilyl (BA) is a key photochemical reaction for elucidating the charge transfer mechanism.^{1,2} BA has two anthracene rings perpendicular to each other in the ground state. When BA is irradiated with the UV light, it is excited to the locally excited (LE) state in which one of the anthracene moieties is electronically excited. In polar solvents, electrons are rearranged between the two anthracene rings and the charge transfer (CT) state is formed. In the charge transfer reaction, the solvation^{3–7} and the internal rotation around the central C–C bond^{8–10} have been considered as vital processes. However, the mechanism of this basic reaction has not yet been fully understood.

Because the intramolecular charge transfer takes place in BA despite the fact that it has no permanent dipole moment in the ground state, the symmetry breaking in the reaction is of great significance for understanding how the CT state is formed in polar solvents. Suppose that a permanent dipole is given to BA by asymmetric substitution. The solvation structure is formed in the ground state to stabilize the dipole. If the charge transfer is controlled by the solvation process, this solvation structure

will affect the charge transfer kinetics of the asymmetric derivatives. However, if the internal rotation from the perpendicular configuration affects the reaction kinetics, the reaction rate is not necessarily affected by the asymmetric substitution.

Previous works have revealed the complicated nature of the substituent effect on the intramolecular charge transfer in BA. The charge transfer proceeded faster in a monochloro-substituted bianthrilyl than in the nonsubstituted one.⁷ It was suggested that the asymmetric configuration of the prepolarized solvation shell formed in the ground state promoted the reaction in the excited state. A transient absorption study of BA adsorbed in porous glass¹¹ indicated an unexpected fast CT formation in the macroscopically nonpolar glass environment. The result suggested symmetry breaking in BA due to the adsorption. No acceleration was observed, however, in the reaction of another polar derivative, carbazolylanthracene, in which an anthracene ring is replaced with a carbazole ring.^{6,9,10} Cyano-substituted bianthrils showed the charge transfer within an excitation pulse duration of 60 fs followed by the solvation and internal rotation processes.^{12,13} Obviously, it is vital to examine the electronic structure of the reactant derivative for fully understanding the reaction mechanism.

Ultrafast spectroscopy is effective in observing the charge transfer reaction of BA, which proceeds in sub-picoseconds to several picoseconds, depending on the solvent. There are several studies on the symmetry breaking effect with systematically prepared symmetric and asymmetric derivatives of BA.^{14–18} To the best of our knowledge, however, there has been no study on the effect of symmetry with ultrafast spectroscopy. In the present study, we prepare BA and three of its derivatives, 10-

* Corresponding author. E-mail: iwata@chem.s.u-tokyo.ac.jp. Fax: +81 3 5841 4540.

[†] Department of Chemistry, School of Science, The University of Tokyo.

[‡] Present address: Department of Chemistry, The Ohio State University, Columbus, OH 43210.

[§] Present address: Department of Chemistry, Georgetown University, Washington, DC 20057.

^{||} University of Hyderabad.

[⊥] Research Centre for Spectrochemistry, School of Science, The University of Tokyo.

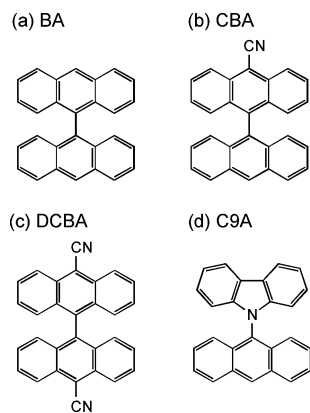


Figure 1. Molecules examined in this study: (a) 9,9'-bianthryl (BA); (b) 10-cyano-9,9'-bianthryl (CBA); (c) 10,10'-dicyano-9,9'-bianthryl (DCBA); (d) 9-(*N*-carbazolyl)anthracene (C9A).

cyano-9,9'-bianthryl (CBA), 10,10'-dicyano-9,9'-bianthryl (DCBA), and 9-(*N*-carbazolyl)anthracene (C9A) (Figure 1). The effects of symmetric and asymmetric substitution on the intramolecular charge transfer reaction are examined.

Among the ultrafast spectroscopies, femtosecond time-resolved near-IR spectroscopy is particularly promising, because it can detect both the LE and CT absorption bands simultaneously.¹⁹ In the near-IR region, the LE band was observed at a similar position as the transient absorption band of S_1 anthracene, while the broad CT band was observed at 1250 nm. We discussed that the broad CT band reflected the interaction between the two aromatic groups. In this study, we reveal that the character of the CT state of the symmetric derivatives is clearly different from the asymmetric ones, based on the observed CT bands in the near-IR region.

Experimental Section

Samples of 10-cyano-9,9'-bianthryl (CBA) and 10,10'-dicyano-9,9'-bianthryl (DCBA) were prepared from their respective mono or dibromo derivative following a method suggested by Muller and Baumgarten.²⁰ The prepared compounds were characterized by ^1H NMR, ^{13}C NMR, and IR spectroscopy. The electronic absorption and fluorescence spectra of the prepared systems were found consistent with the literature. The carbazolyl-substituted derivative, 9-(*N*-carbazolyl)anthracene (C9A), was synthesized by the fusion of carbazole (1.0 mol) and 9-bromoanthracene (1.2 mol) at 280 °C for 2.5 h and was

purified by column chromatography (5% chloroform in hexane). It was then recrystallized from a mixture of benzene and chloroform at room temperature. The product was confirmed by ^1H , ^{13}C NMR, and UV–visible spectroscopy. Nonsubstituted 9,9'-bianthryl (BA) was synthesized as reported by Magnus et al.²¹ Anthracene (>99%) was purchased from Wako Pure Chemical Industries Inc. and was used as received. The cyano-substituted monomer unit, 9-cyanoanthracene (CA, 95%), was purchased from Tokyo Kasei Kogyo Co., Ltd., and was used after being recrystallized from toluene and sublimed under vacuum at 378 K. Heptane (HPLC grade) and acetonitrile (spectrograde) were purchased from Kanto Kagaku Co. and were used without further purification.

Steady-state UV–visible absorption spectra were measured by a UV–visible–near-IR absorption spectrometer (Hitachi U-3500). Femtosecond time-resolved near-IR absorption spectra were obtained with the pump–probe technique. Details of the spectrometer were described elsewhere.¹⁹ For recording the time-resolved absorption spectra of BA and C9A, the wavelength of the pump light was set at 393 nm, using the second harmonic of the amplified Ti:sapphire laser. The second harmonic was tuned to 410 nm for the photoexcitation of CBA, DCBA, and CA. For the measurement of anthracene, the third harmonic (262 nm) was used as the pump light. At the sample point, the pulse energy and beam diameter (at the $1/e^2$ intensity of the peak) of the pump light were 3 μJ and ≈ 0.5 mm. The angle between the polarization of the pump and probe light was fixed at 54.7°, so that rotational relaxation did not affect the measurement. All of the experiments were performed at room temperature. The concentrations of BA, C9A, CBA, and DCBA in acetonitrile were 5×10^{-4} , 1×10^{-3} , 1×10^{-4} , and 5×10^{-5} mol dm^{-3} , respectively. The concentration of anthracene in heptane was 2×10^{-3} mol dm^{-3} . The concentration of CA in acetonitrile was 5×10^{-4} mol dm^{-3} . The sample solutions were circulated through a 2-mm-thick quartz cell.

Results and Discussion

Electronic Structure of the LE State. Steady-state absorption spectra were recorded in the wavelength region between 250 and 800 nm. All of the derivatives showed an absorption band in the range 300–450 nm. The results are represented in Figure 2a. The spectra of the asymmetric derivatives, CBA and C9A, are well-explained as the superposition of the two monomer units. Their LE states have the character of either of

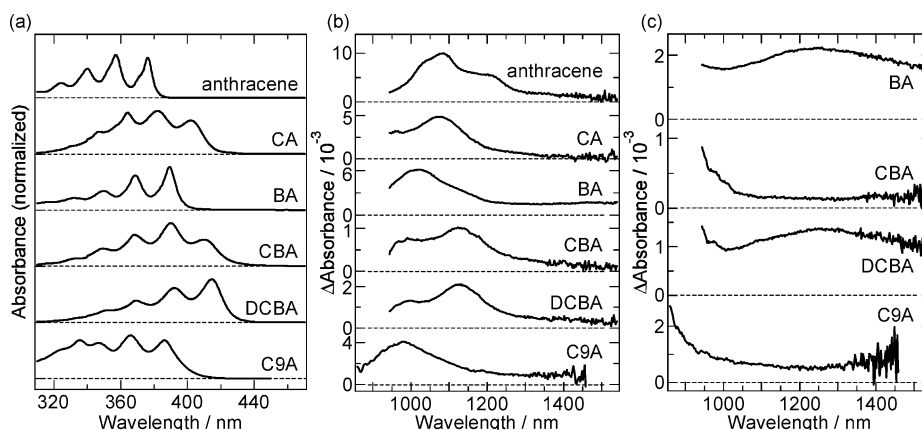


Figure 2. (a) Steady-state absorption spectra of BA, its derivatives, and their monomer units which are likely to be photoexcited. All of the spectra are normalized at the absorption maximum. (b) Time-resolved near-IR absorption spectra of BA and its derivatives at 0 ps after the photoexcitation. Transient absorption spectra of anthracene and CA in the S_1 state are also shown. (c) Time-resolved near-IR absorption spectra of BA and its derivatives at 3 ps after the photoexcitation.

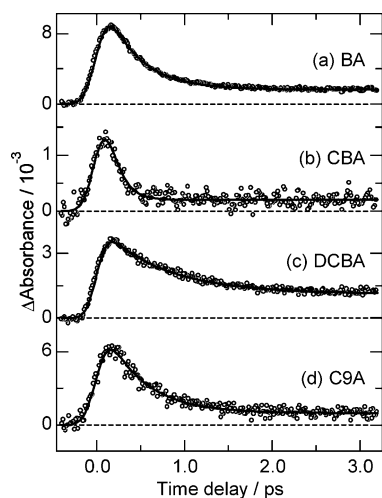


Figure 3. Time dependence of absorbance changes of BA and its derivatives at the LE peak position: (a) BA; (b) CBA; (c) DCBA; (d) C9A. The data points are represented by open circles. The best results of the fitting analysis are shown with solid curves.

the monomer units which is locally excited at the moment of the photoexcitation.

The steady-state absorption spectra indicate that the monomer unit which has the lower excitation energy in the derivatives is selectively photoexcited when they are irradiated at the wavelength corresponding to the 0–0 transition. From the spectra of the monomer compounds, we can estimate that the S_1 energy level of anthracene is below that of carbazole by 3320 cm^{-1} and above that of CA by 1730 cm^{-1} . These energy differences allow a selective photoexcitation with the femtosecond pump pulses, which has an energy width of $\approx 200\text{ cm}^{-1}$. We assume that the anthracene ring is electronically excited in BA and C9A by the irradiation of the pump light, whereas the cyanoanthracene (CA) ring is excited in CBA and DCBA.

Near-IR absorbance changes of BA and its derivatives induced by photoexcitation were recorded in the polar solvent acetonitrile. The femtosecond time-resolved near-IR absorption spectra showed two temporal components, as presented in Figure 2b and c. At 0 ps (Figure 2b), each BA derivative exhibits an absorption band that is assigned to the LE-state absorption.¹⁹ The observed LE bands are classified into two groups. BA and C9A show the LE bands at 1020–980 nm, respectively, whereas CBA and DCBA show those at around 1150 nm. This result is consistent with the assumption, as mentioned above, that the anthracene ring is photoexcited in BA and C9A and that the CA ring is photoexcited in CBA and DCBA.

The charge transfer rate is estimated by plotting the absorbance change at the peak position of the LE band against time delay. The obtained time dependence is shown in Figure 3. There was no difference between the decay curves for BA recorded with pump energies of 3 and $13\ \mu\text{J}$. Time constants of the LE decay curves were determined by least-squares fitting with a single-exponential function. The obtained time constants are 0.38 ± 0.01 , 0.15 ± 0.02 , 0.6 ± 0.1 , and 0.44 ± 0.02 ps for BA, CBA, DCBA, and C9A, respectively. The observed decay dynamics is not simply explained by the difference of the symmetry of substitution. The asymmetric substitution results in a faster (CBA) or slower (C9A) charge transfer rate, while the symmetric substitution decelerates the reaction by 60%. The obtained time constants probably indicate that the reaction kinetics is strongly influenced by the electronic structure of the reactants in the LE and CT states. It seems difficult to extract information on the effect of the solvation or the internal rotation process on the decay kinetics.

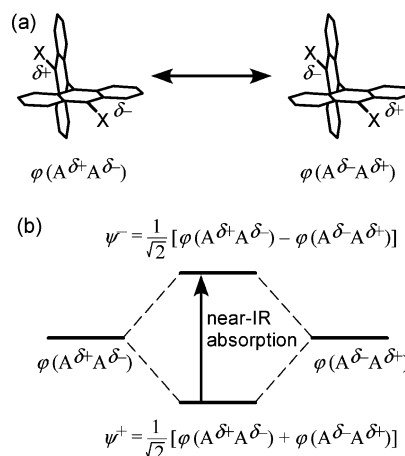


Figure 4. (a) Resonance structure of the symmetric BA derivatives in the CT state. X = H or CN. (b) The schematic diagram of the charge resonance transition.

The CT Absorption Bands Dependent on the Symmetry of Substitution.

After 3 ps from the photoexcitation, absorption bands assigned to the CT absorption¹⁹ appeared, while the LE bands decayed and disappeared. The results are shown in Figure 2c. The obtained CT absorption bands are classified into two groups, based on their band shapes. BA and DCBA have broad CT absorption bands centered at 1250 nm, whereas CBA and C9A show absorption which monotonically decreases as the probe wavelength becomes longer. This distinction clearly shows that the shape of the CT band, unlike the LE band, is dependent on the symmetry of the derivatives.

According to the transient visible absorption^{7,22} and coherent anti-Stokes Raman spectroscopy (CARS)²³ studies, BA and its derivatives had a CT absorption band centered at around 690 nm. It was assigned to the radical absorption band, because the anion²⁴ or cation²⁵ radical of anthracene showed an absorption band in this wavelength region. A distinct near-IR band observed only for the symmetric derivatives at 1250 nm, however, is not consistent with the charge separated state model in which the CT state is described as the summation of the cation radical and the anion radical of the anthracene monomer. In the charge separation model, the 1250 nm band should originate in either the cation or anion radical of the anthracene moiety. Because CBA has an electron withdrawing group connected to the anthracene monomer, it will show the absorption bands of the anthracene cation radical if the CT state is the charge separated state. Similarly, because C9A has an electron donating group, its CT state will show the anthracene anion radical bands. However, neither of them showed the 1250 nm band. Therefore, the 1250 nm band is not explained as the absorption of the cation or anion radical of anthracene. The charge separated state is not a good model for the excited CT state of BA.

In order to explain why only the symmetric BA derivatives show the near-IR broad CT absorption bands, we adopt a model based on the charge resonance mechanism. The schematic diagram of the CT-state stabilization in this model is shown in Figure 4. Two equivalent states, $(\text{ANT})^{\delta+}-(\text{ANT})^{\delta-}$ and $(\text{ANT})^{\delta-}-(\text{ANT})^{\delta+}$, where ANT stands for the anthryl group, can mix with each other by the charge resonance between them. Wave functions of the CT states, ψ^{\pm} , are expressed by the linear combination of the wave functions of $(\text{ANT})^{\delta+}-(\text{ANT})^{\delta-}$ and $(\text{ANT})^{\delta-}-(\text{ANT})^{\delta+}$

$$\psi^{\pm}(\text{CT}) = \frac{1}{\sqrt{2}} \{ \varphi(\text{A}^{\delta+}\text{A}^{\delta-}) \pm \varphi(\text{A}^{\delta-}\text{A}^{\delta+}) \} \quad (1)$$

where $\varphi(A^{\delta+}A^{\delta-})$ and $\varphi(A^{\delta-}A^{\delta+})$ are the wave functions of $(ANT)^{\delta+}-(ANT)^{\delta-}$ and $(ANT)^{\delta-}-(ANT)^{\delta+}$, respectively. With regard to the axis along the central C–C bond, ψ^+ and ψ^- have the gerade and ungerade symmetries. The transition between ψ^+ and ψ^- is, therefore, optically allowed and has the transient dipole moment along the central C–C bond. The broad CT absorption band of the symmetric derivatives can be attributed to the transition from ψ^+ to ψ^- . The observed CT bandwidth of BA and DCBA extends over 3000 cm^{-1} , which is common in many charge resonance bands.

The charge resonance between two fully electron-transferred states, $(ANT)^+-(ANT)^-$ to $(ANT)^--(ANT)^+$, requires the rearrangement of two electrons. The two-electron transfer is not simply described, if ψ^+ and ψ^- are expressed as products of one-electron wave functions. Because the product of one-electron wave functions is generally a good approximation for expressing a molecular wave function, the probability of the two-electron transfer should be sufficiently small. Apparently, the electrons are not fully transferred from one moiety to the other. Okada and his collaborators²⁶ suggested that BA did not reach the complete charge separation at above 165 K. Our model is consistent with their experimental results at room temperature.

Our assignment of the near-IR absorption band to the charge resonance transition may appear inconsistent with the previous assignment of the visible absorption band to the radical ion species. However, it has been reported that the anthracene dimer anion shows both the charge resonance band and absorption bands similar to the radical ion.²⁴ The similarity between the visible absorption band of BA at 690 nm and the anthracene radical anion or cation band at around 710 nm may be explained by similar charge resonance interaction between the initial and final states of the visible transition.

The CT bands of the symmetric derivatives are centered at 1250 nm. The energy gap between the two states generated by the charge resonance is 8000 cm^{-1} . If we represent the interaction by the exchange time between the two equivalent states, $(ANT)^{\delta+}-(ANT)^{\delta-}$ and $(ANT)^{\delta-}-(ANT)^{\delta+}$, it will be 4 fs. The ultrafast exchange will prohibit the orientation or translation solvation. It is noteworthy that the value of the solvation energy is not consistent with the charge resonance between $(ANT)^{\delta+}-(ANT)^{\delta-}$ and $(ANT)^{\delta-}-(ANT)^{\delta+}$ in the “fixed” solvation shell. In acetonitrile, the stabilization energy of $(ANT)^{\delta+}-(ANT)^{\delta-}$ by the solvation is estimated to be 9.3 kcal mol^{-1} , or 3300 cm^{-1} , from the dynamic Stokes shift values.⁵ At the same time, $(ANT)^{\delta-}-(ANT)^{\delta+}$ becomes unstable by 3300 cm^{-1} . The total energy gap between $(ANT)^{\delta+}-(ANT)^{\delta-}$ and $(ANT)^{\delta-}-(ANT)^{\delta+}$ amounts to 6600 cm^{-1} . This energy gap does not allow charge resonance between the two equivalent states. It is possible that ultrafast fluctuation of solvent molecules, probably corresponding to the electronic polarizability, is significant for the charge resonance, or CT formation process in the symmetric BA derivatives. The flip-flop dipole reversal of BA in nonpolar solvents was proposed by the microwave conductivity measurement.^{18,27,28} The reversal time was estimated to be ~ 2 ps in alkanes.¹⁸ This model is similar to our proposition that the exchange occurs between the two equivalent charge separated states, although our estimation of the exchange in acetonitrile is much faster.

The asymmetric BA derivatives, CBA and C9A, do not show the broad CT bands. This is understandable because the charge resonance between two nonequivalent states in the asymmetric derivatives is expected to be negligible. In the case of CBA, the formation energies of $(ANT)^{\delta+}-(CA)^{\delta-}$ and $(ANT)^{\delta-}-(CA)^{\delta+}$ are estimated to be 6.17 eV (49 800 cm^{-1}) and 7.27

eV (58 600 cm^{-1}), respectively, from the ionization energy of anthracene and CA in the gas phase^{29,30} and from their electron affinity.^{31,32} The large energy gap of 8800 cm^{-1} between the two states does not cause the resonance interaction between the two rings. Thus, the CT-state stabilization mechanism of the symmetric bianthryls is different from that of the asymmetric ones. The mechanism of the intramolecular charge transfer reaction can also be different between them, because it contains the stabilization process of the photoproduct. The charge resonance in the CT state of symmetric derivatives can be a key factor of the charge transfer reaction in acetonitrile, in addition to the possible solvation and internal rotation processes.

Acknowledgment. This work is supported by Grant-in-Aid for Creative Scientific Research (no. 11NP0101) and Grant-in-Aid for Scientific Research (B) (no. 15350005) from Japan Society for the Promotion of Science (JSPS) and Grant-in-Aid for Scientific Research on Priority Areas (area 417, no. 15033219) from the Ministry of Education, Culture, Sports, Science and Technology (MEXT) of the Japanese Government. This work is also supported by the Joint Research Project under the India-Japan Scientific Cooperative Programme funded jointly by JSPS and Department of Science and Technology (DST), Government of India.

References and Notes

- (1) Schneider, F.; Lippert, E. *Ber. Bunsen-Ges. Phys. Chem.* **1968**, *72*, 1155.
- (2) Schneider, F.; Lippert, E. *Ber. Bunsen-Ges. Phys. Chem.* **1970**, *74*, 624.
- (3) Barbara, P. F.; Jarzaba, W. *Adv. Photochem.* **1990**, *15*, 1.
- (4) Kahlow, M. A.; Kang, T. J.; Barbara, P. F. *J. Phys. Chem.* **1987**, *91*, 6452.
- (5) Kang, T. J.; Kahlow, M. A.; Giser, D.; Swallen, S.; Nagarajan, V.; Jarzaba, W.; Barbara, P. F. *J. Phys. Chem.* **1988**, *92*, 6800.
- (6) Kang, T. J.; Jarzaba, W.; Barbara, P. F.; Fonseca, T. *Chem. Phys.* **1990**, *149*, 81.
- (7) Mataga, N.; Yao, H.; Okada, T.; Rettig, W. *J. Phys. Chem.* **1989**, *93*, 3383.
- (8) Mataga, N.; Nishikawa, S.; Okada, T. *Chem. Phys. Lett.* **1996**, *257*, 327.
- (9) Jurczok, M.; Plaza, P.; Martin, M. M.; Meyer, Y. H.; Rettig, W. *Chem. Phys.* **2000**, *253*, 339.
- (10) Jurczok, M.; Gustavsson, T.; Mialocq, J.-C.; Rettig, W. *Chem. Phys. Lett.* **2001**, *344*, 357.
- (11) Tsuboi, Y.; Kumagai, T.; Shimizu, M.; Itaya, A.; Schweitzer, G.; De Schryver, F. C.; Asahi, T.; Masuhara, H.; Miyasaka, H. *J. Phys. Chem. A* **2002**, *106*, 2067.
- (12) Jurczok, M.; Plaza, P.; Rettig, W.; Martin, M. M. *Chem. Phys.* **2000**, *256*, 137.
- (13) Kovalenko, S. A.; Lustres, J. L. P.; Ernsting, N. P.; Rettig, W. *J. Phys. Chem. A* **2003**, *107*, 10228.
- (14) Müller, S.; Heinze, J. *Chem. Phys.* **1991**, *157*, 231.
- (15) Elich, K.; Lebus, S.; Wortmann, R.; Petzke, F.; Detzer, N.; Liptay, W. *J. Phys. Chem.* **1993**, *97*, 9947.
- (16) Catalán, J.; Díaz, C.; López, V.; Pérez, P.; Claramunt, R. M. *J. Phys. Chem.* **1996**, *100*, 18392.
- (17) Zachariasse, K. A.; Grobys, M.; von der Haar, Th.; Hebecker, A.; Il'ichev, Yu. V.; Jiang, Y.-B.; Morawski, O.; Kühnle, W. *J. Photochem. Photobiol., A* **1996**, *102*, 59.
- (18) Piet, J. J.; Schuddeboom, W.; Wegewijs, B. R.; Grozema, F. C.; Warman, J. M. *J. Am. Chem. Soc.* **2001**, *123*, 5337.
- (19) Takaya, T.; Hamaguchi, H.; Kuroda, H.; Iwata, K. *Chem. Phys. Lett.* **2004**, *399*, 210.
- (20) Müller, U.; Baumgarten, M. *J. Am. Chem. Soc.* **1995**, *117*, 5840.
- (21) Magnus, A.; Hartmann, H.; Becker, F. *Z. Phys. Chem.* **1951**, *197*, 75.
- (22) Nakashima, N.; Murakawa, M.; Mataga, N. *Bull. Chem. Soc. Jpn.* **1976**, *49*, 854.
- (23) Matsunuma, S.; Kamisuki, T.; Adachi, Y.; Maeda, S.; Hirose, C. *Spectrochim. Acta* **1988**, *44A*, 695.
- (24) Shida, T.; Iwata, S. *J. Chem. Phys.* **1972**, *56*, 2858.
- (25) Szczepanski, J.; Vala, M.; Talbi, D.; Parisel, O.; Ellinger, Y. *J. Chem. Phys.* **1993**, *98*, 4494.

(26) Nishiyama, K.; Honda, T.; Okada, T. *Acta Phys. Pol., A* **1998**, *94*, 847.

(27) Toublanc, D. B.; Fessenden, R. W.; Hitachi, A. *J. Phys. Chem.* **1989**, *93*, 2893.

(28) Warman, J. M.; Schuddeboom, W.; Jonker, S. A.; de Haas, M. P.; Paddon-Row, M. N.; Zachariasse, K. A.; Launay, J.-P. *Chem. Phys. Lett.* **1993**, *210*, 397.

(29) Hager, J. W.; Wallace, S. C. *Anal. Chem.* **1988**, *60*, 5.

(30) Klasinc, L.; Kovac, B.; Schoof, S.; Gusten, H. *Croat. Chem. Acta* **1978**, *51*, 307.

(31) Schiedt, J.; Weinkauff, R. *Chem. Phys. Lett.* **1997**, *266*, 201.

(32) Heinis, T.; Chowdhury, S.; Kebarle, P. *Org. Mass Spectrom.* **1993**, *28*, 358.